Modeling Biocide Action Against Biofilms

Philip S. Stewart,[1]* Martin A. Hamilton,[2] Brian R. Goldstein, and Brian T. Schneider[2]
Center for Biofilm Engineering, [1]Department of Chemical Engineering and [2]Department of Mathematical Sciences, Montana State University, Bozeman, Montana 59717

Received January 31, 1995/Accepted September 20, 1995

A phenomenological model of biocide action against microbial biofilms was derived. Processes incorporated in the model include bulk flow in and out of a well-mixed reactor, transport of dissolved species into the biofilm, substrate consumption by bacterial metabolism, bacterial growth, advection of cell mass within the biofilm, cell detachment from the biofilm, cell death, and biocide concentration-dependent disinfection. Simulations were performed to analyze the general behavior of the model and to perform preliminary sensitivity analysis to identify key input parameters. The model captured several general features of antimicrobial agent action against biofilms that have been observed widely by experimenters and practitioners. These included (1) rapid disinfection followed by biofilm regrowth, (2) slower detachment than disinfection, and (3) reduced susceptibility of microorganisms in biofilms. The results support the plausibility of a mechanism of biofilm resistance in which the biocide is neutralized by reaction with biofilm constituents, leading to a reduction in the bulk biocide concentration and, more significantly, biocide concentration gradients within the biofilm. Sensitivity experiments and analyses identified which input parameters influence key response variables. Each of three response variables was sensitive to each of the five input parameters, but they were most sensitive to the initial biofilm thickness and next most sensitive to the biocide disinfection rate coefficient. Statistical regression modeling produced simple equations for approximating the response variables for situations within the range of conditions covered by the sensitivity experiment. The model should be useful as a tool for studying alternative biocide control strategies. For example, the simulations suggested that a good interval between pulses of biocide is the time to minimum thickness.
Key words: biofilm • biocide • disinfection • reaction-diffusion

INTRODUCTION

Microbial biofilms will form on virtually any surface that is in contact with water. Even though biofilms are often quite thin (less than 1 mm thick) they can cause serious problems. Examples of the detrimental consequences of biofilm formation include energy losses and downtime in cooling water systems,[34] coliform outbreaks in drinking water distribution systems,[6] corrosion and biodeterioration of process equipment and pipelines,[15] pathogen contamination of food processing equipment,[7] degradation of product quality in the manufacture of paper and liquid consumer products,[16] fouling of reverse osmosis membranes,[27] plugging of water injection wells,[15] degradation of metal-working fluid properties,[20] degradation of swimming pool appearance and hygiene,[13] dental caries and periodontal disease,[22] and recalcitrant infections associated with indwelling medical devices.[11]

In all of these systems, antimicrobial agents are routinely used to control the biofilm. Biofilm microorganisms, however, are usually found to be much more difficult to eradicate than are their planktonic counterparts.[11] For example, antibiotics may suppress the symptoms of a biofilm infection by killing planktonic organisms, but once chemotherapy ceases, the biofilm quickly regrows and the infection manifests itself anew. Biofilm regrowth in industrial systems is also well known.[25] From a practical standpoint, one would like to have ways to subvert biofilm resistance, or at least cope with it knowledgeably. It would also be nice to have design methods for anticipating the time required for biofilm regrowth and for selecting efficient antimicrobial dosing protocols. The scientific challenges to achieving these goals are to understand fundamental physical, chemical, and biological phenomena that underlie biofilm resistance and to develop quantitative descriptions of them so that the process can be engineered and optimized.

Engineering biofilm control is a formidable task because the action of an antimicrobial on biofilm involves the complex interaction of multiple processes. Among the constituent phenomena that must be considered are planktonic and biofilm growth, substrate utilization, biofilm detachment, microbial disinfection, bulk flow through the system, diffusive transport within the biofilm, consumption of biocide or antibiotic by reaction with biomass, and particulate dynamics in the biofilm. Additional processes that might confound the problem include corrosion, accumulation of abiotic particulates in the biofilm, and mutation and adaptation.

Precisely because of its complexity, the problem of antimicrobial control of biofilm is one that invites mathematical modeling. Modeling is one way to organize and

* To whom all correspondence should be addressed.

CCC 0006-3592/96/040445-11

integrate phenomena systematically. A model is a means of both formulating a hypothesis and exploring its implications. It can also be a tool for interpreting experimental data that might otherwise be difficult to analyze. At the Center for Biofilm Engineering, the model described in this article has been used to design experiments and to evaluate the theoretical plausibility of various resistance mechanisms.[32] Ultimately, using a model could be the most effective way of performing design and scale-up tasks, such as developing optimal biocide dosage protocols for a particular system.

Earlier modeling studies have considered various aspects of biofilm disinfection, but none has coupled complete descriptions of biofilm and bulk dynamics. Models of chlorine decay in drinking and cooling water systems exist,[1,3,29] but they neglect the biofilm or treat it as a single compartment. Nichols and co-workers[23,24] have modeled antibiotic penetration into a microbial colony but did not consider the killing process or bulk fluid dynamics. Characklis[8] outlined a pipeline model that incorporated axial plug flow, radial eddy diffusion, and biocide reaction with biofilm and bulk water.[8] None of these models included analysis of the population dynamics in the biofilm, though multispecies biofilm models exist.[21,36] In this article, we describe a model of biofilm–biocide interaction that integrates features of bulk fluid dynamics, biofilm dynamics, and the coupled reaction and diffusion of biocide and substrate.

The purpose of this article is to introduce a phenomenological model of biocide action against biofilms. Specific objectives are to illustrate the general behavior of the model and compare it to experimental observations reported in the literature and perform preliminary sensitivity analyses to identify key input parameters.

MODELING

A phenomenological computer model of biofilm dynamics was adapted to describe the activity of an antimicrobial agent on biofilm.[32] This model was developed by researchers at the Center for Biofilm Engineering based on the conceptual and mathematical formulation described by Wanner and Gujer.[36] Its central principle is conservation of mass, which is applied to bulk liquid and biofilm compartments. The equations for the bulk liquid compartment simulate the dynamics of a chemostat, which is a well-mixed, constant-volume, continuous-flow reactor. Coupled to the equations describing bulk liquid constituents are separate balance equations pertaining to transport and reaction processes within the biofilm. The biofilm is treated as a uniformly thick planar aggregate whose composition changes only in the direction perpendicular to the substratum. This conceptual view of the biofilm permits a one-dimensional mathematical model. System geometry is schematically depicted in Figure 1.

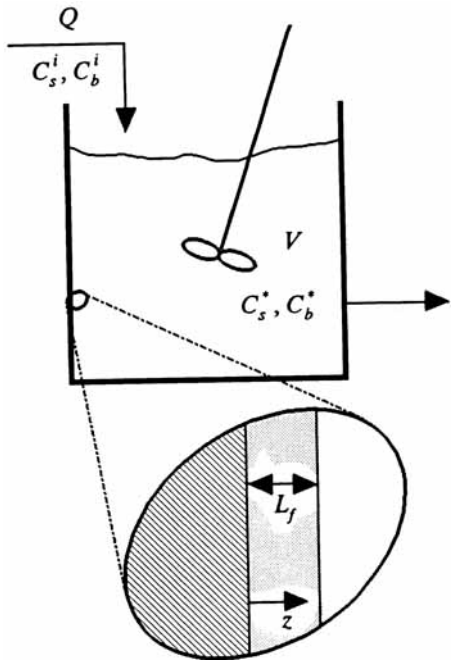

Figure 1. System compartments and geometry. A biofilm of uniform thickness L_f grows on the wall of a continuous-flow stirred-tank reactor.

Processes incorporated in the model include bulk flow in and out of the reactor, transport of dissolved solutes into the biofilm, substrate consumption by bacterial metabolism, bacterial growth, advection of cell mass within the biofilm, cell detachment from the biofilm, cell death, and disinfection (Table I). The mathematical model comprises differential material balances containing terms representing these processes along with associated initial and boundary conditions. A special feature of the model is the capacity to vary the feed concentra-

Table I. Processes incorporated in the model.

Process	Submodel
Bulk fluid flow in and out of reactor	Continuous-flow stirred-tank reactor
Transport of dissolved species within biofilm	Fickian diffusion
External mass transfer	Concentration boundary layer of constant thickness
Substrate consumption	Proportional via constant yield coefficient to biomass growth
Growth	Monod dependence on substrate concentration
Death	First-order decay (not biocide dependent)
Transport of cells within biofilm	Advection due to growth
Detachment	Proportional to biofilm thickness squared
Disinfection	Proportional to local biocide concentration

tion of dissolved species according to a programmed schedule. This permits various biocide dosing protocols to be readily investigated. The EAWAG model AQUASIM could also be used to implement such simulations.

Biofilm Compartment

A biofilm consisting of a single microbial species is considered. Within the biofilm, the concentrations of live cells, dead cells, growth substrate, and biocide are analyzed. Although there is only one microbial species, a multispecies model is required since there are two cell states. The concentrations of cells inside the biofilm are expressed in terms of volume fractions. Volume fractions are converted to mass units through the intrinsic cell density, ρ_x, which is assumed to be the same for both live and dead cells. Since the fraction of biofilm volume occupied by all cells combined is assumed constant, the concentrations of live and dead cells are subject to the constraint

$$\varepsilon_a + \varepsilon_i = \varepsilon_c \tag{1}$$

The balance on live cells is

$$\frac{\partial \varepsilon_a}{\partial t} = \frac{\mu_{\max} C_s}{K_s + C_s} \varepsilon_a - \frac{\partial}{\partial z}(v\varepsilon_a) - b\varepsilon_a - k_r C_b \varepsilon_a \tag{2}$$

where the terms represent, from left to right, accumulation, growth, advection, death, and disinfection. The substrate concentration dependence of microbial growth is modeled by Monod kinetics. Both disinfection and death processes convert live cells to dead cells with one-to-one stoichiometry. Whereas disinfection is proportional to the local biocide concentration, death is modeled as a simple first-order decay process that is independent of biocide concentration. Including death helped stabilize the numerical solution by precluding extremely small dead cell concentrations. The biofilm is assumed to be composed entirely of live cells initially; the initial condition associated with Equation (2) is thus

$$\varepsilon_a = \varepsilon_c \quad \text{at } t = 0 \text{ for } 0 \le z \le L_f^0 \tag{3}$$

As cell volume is created in the biofilm due to growth, cells displace their neighbors away from the substratum. Live and dead cells at the same point in the biofilm move with the same velocity. The advective velocity must satisfy

$$\frac{\partial v}{\partial z} = \frac{\mu_{\max} C_s}{K_s + C_s} \frac{\varepsilon_a}{\varepsilon_c} \tag{4}$$

subject to the boundary condition

$$v = 0 \quad \text{at } z = 0 \text{ for } t > 0 \tag{5}$$

Growth and detachment[31] processes change the thickness of the biofilm according to

$$\frac{dL_f}{dt} = v|_{z=L_f} - k_d L_f^2 \tag{6}$$

with the initial condition

$$L_f = L_f^0 \quad \text{at } t = 0 \tag{7}$$

The concentration of growth limiting substrate in the biofilm is described by a reaction–diffusion equation

$$\frac{\partial C_s}{\partial t} = D_s \tau \frac{\partial^2 C_s}{\partial z^2} - \frac{\mu_{\max}}{Y_{xs}} \frac{C_s}{K_s + C_s} \varepsilon_a \rho_x \tag{8}$$

in which it is assumed that only live cells consume substrate. Molecular diffusion is the only transport mechanism for dissolved species within the biofilm. Reduction in the effective diffusion coefficient inside the biofilm is allowed through the parameter τ. The initial condition is

$$C_s = C_s^i \quad \text{at } t = 0 \text{ for } 0 \le z \le L_f^0 \tag{9}$$

Boundary conditions on Equation (8) impose a matching flux condition at the biofilm–bulk fluid interface,

$$\tau \frac{\partial C_s}{\partial z}\Big|_{z=L_f} = \frac{C_s^* - C_s|_{z=L_f}}{L_L} \quad \text{for } t \ge 0 \tag{10}$$

and a no-flux condition at the substratum,

$$\frac{\partial C_s}{\partial z}\Big|_{z=0} = 0 \quad \text{for } t \ge 0 \tag{11}$$

Biocide reacts with biomass, and so it is also subject to a reaction–diffusion interaction. The balance on biocide is

$$\frac{\partial C_b}{\partial t} = D_b \tau \frac{\partial^2 C_b}{\partial z^2} - k_r C_b \varepsilon_c \rho_x \tag{12}$$

The formulation of Equation (12) assumes that the biocide reacts with live and dead cells at the same rate. Initial and boundary conditions are analogous to those for the growth substrate,

$$C_b = 0 \quad \text{at } t = 0 \text{ for } 0 \le z \le L_f^0 \tag{13}$$

$$C_b = C_b^* \quad \text{at } z = L_f \text{ for } t > 0 \tag{14}$$

$$\frac{\partial C_b}{\partial z} = 0 \quad \text{at } z = 0 \text{ for } t > 0 \tag{15}$$

Bulk Fluid Compartment

Differential material balances on the bulk fluid compartment account for flow in and out of the chemostat, bulk phase reactions, and the net reaction arising from the biofilm. The balances on live cells is

$$\frac{dX_a^*}{dt} = \frac{\mu_{\max} C_s^*}{K_s + C_s^*} X_a^* - bX_a^* - k_b X_a^* C_b^* + k_d \varepsilon_a|_{z=L_f} \rho_x L_f^2 \frac{A}{V} - \frac{Q}{V} X_a^* \tag{16}$$

From left to right, the terms in this equation account for accumulation, bulk phase growth, bulk phase death, bulk phase disinfection, biofilm detachment of live cells, and flow out of the reactor. The balance on dead cells is similar except for the absence of the growth term:

$$\frac{dX_i^*}{dt} = bX_a^* - k_b X_a^* C_b^* + k_d \varepsilon_i|_{z=L_f} \rho_x L_f^2 \frac{A}{V} - \frac{Q}{V} X_i^* \quad (17)$$

The reactor bulk fluid is initially free of particulates:

$$X_a^* = X_i^* = 0 \quad \text{at } t = 0 \quad (18)$$

Substrate is continually supplied in the influent but is consumed by live cells in the bulk fluid and biofilm, giving

$$\frac{dC_s^*}{dt} = \frac{Q}{V}(C_s^i - C_s^*) - \frac{\mu_{\max} C_s^*}{K_s + C_s^*} X_a^* - D_s \tau \frac{dC_s}{dz}\Big|_{z=L_f} \frac{A}{V} \quad (19)$$

with

$$C_s^* = C_s^i \quad \text{at } t = 0 \quad (20)$$

The biocide concentration in the bulk is similarly

$$\frac{dC_b^*}{dt} = \frac{Q}{V}(C_b^i - C_b^*) - k_r C_b (X_a^* + X_i^*) - D_b \tau \frac{dC_b}{dz}\Big|_{z=L_f} \frac{A}{V} \quad (21)$$

with a stepped dose of biocide delivered in the influent according to

$$C_b^i(t) = \begin{cases} 0 & t < t_1 \\ C_b^i & t_1 \le t \le t_2 \\ 0 & t > t_2 \end{cases} \quad (22)$$

with

$$C_b^* = 0 \quad \text{at } t = 0 \quad (23)$$

Numerical Solution Technique

The nonlinear system of partial differential equations was solved numerically using a variable step size trapezoidal integration scheme with Newton iterations. This method is stable in the range of parameters studied in this article. The method handles biocide concentration step changes without difficulty.

METHODS

Case Studies

The effects of an antimicrobial agent on a microbial biofilm were simulated by adapting a mathematical model of biofilm dynamics to incorporate programmable dosing of a reactive disinfectant. To investigate the general behavior of the model and its sensitivity to selected input parameter values, 243 simulations were conducted by varying five input parameters through three values each (Table II). The five varied parameters were initial biofilm thickness (L_f), influent biocide concentration (C_b), biocide dose duration (t_b), biocide disinfection rate coefficient (k_b), and biocide reaction rate coefficient (k_r). These were selected to vary because of their suspected importance and considerable uncertainty in their values (L_f, k_b, k_r) or because they are controllable parameters (C_b, t_b). Parameter values and ranges were chosen by reference to experimental systems,[9,10,28,30,33] typical values,[2,26,37] and opinion of experts affiliated with the Center for Biofilm Engineering. In one set of runs, repeated dose protocols of various biocide concentrations and dosing intervals were simulated.

Table II. Parameter input values for biofilm modeling.

Parameter	Symbol	Value
Maximum specific growth rate	$\mu_{\max}$	7.5 d^{-1}
Specific death rate	b	0.01 d^{-1}
Yield coefficient	Y_{xs}	0.45 g g^{-1}
Monod coefficient	K_s	2.55 g m^{-3}
Cell volume fraction	ε_c	0.115
Cell intrinsic density	ρ_x	30,000 g m^{-3}
Initial biofilm thickness	L_f	5, 50, 500 μm
Concentration boundary layer thickness	L_L	105 μm
Substrate influent concentration	C_s	8.0 g m^{-3}
Biocide influent concentration	C_b	1, 2, 4 g m^{-3}
Biocide dose duration	t_b	1, 2, 4 h
Substrate diffusion coefficient	D_s	5.7×10^{-4} m^2 d^{-1}
Biocide diffusion coefficient	D_b	1.5×10^{-4} m^2 d^{-1}
Biofilm/bulk diffusivity ratio	τ	0.8
Detachment rate coefficient	k_d	m^{-1} d^{-1}
Surface-area-to-volume ratio	A/V	10 m^{-1}
Dilution rate	Q/V	10 d^{-1}
Biocide disinfection rate coefficient	k_b	75, 300, 1200 m^3 $g^{-1}d^{-1}$
Biocide reaction rate coefficient	k_r	30, 60, 120 m^3 $g^{-1}d^{-1}$

Sensitivity Analysis

Response variables used to measure biocide efficacy included:

- reduction in biofilm viable cell numbers, as given by the minimum value of the ratio of viable cell areal density to initial viable cell areal density on the $\log_{10}$ scale (denoted by LMV for log minimum viability);
- time in hours to minimum biofilm thickness (denoted by TMT); and
- time in hours for biofilm thickness to recover to 99% of its steady-state value (denoted by TR99).

These three variables provide measures of efficacy that relate to different practical aspects of biofilm control. The most commonly applied assay in practice is scraping, followed by disaggregation and plating. To facilitate comparison to this traditional measure, the areal density of viable cells normalized to its initial value was calculated according to

$$\frac{X_{vb}}{X_{vb}^0} = \frac{\int_0^{L_f} \varepsilon_a \, dz}{\varepsilon_c L_f^0} \quad (24)$$

The response variable LMV was then taken as the base 10 logarithm of the value calculated by Equation (24).

In many biofouling problems, the extent to which biomass is removed may be more significant than the degree of disinfection achieved. In this case, total biomass or biofilm thickness is a better measure. We recorded the reduction in biofilm thickness from its initial value [$L_f(t = \text{TMT})/L_f^0$] and the time at which this minimum thickness was reached (TMT). The recovery time is valuable for the purpose of deciding when to add the next biocide dose. To this end, the time required for the biofilm to recover to 99% of its initial value was recorded.

Statistical analyses and graphs were used to interpret data from the simulation experiment. The graphs showed (i) the relationships between each response variable and each input parameter and (ii) the associations between each pair of response variables. The statistical analyses entail regression and correlation calculations, statistics commonly used in computer model sensitivity studies.[5,18,19] A nonlinear least squares regression model for each response variable was constructed to approximate the computer simulation value of that response variable. The regression model was a relatively simple function of the five input parameter values. The quality of the regression model was measured by the correlation coefficient between the predicted value and the corresponding computer simulation value across the 243 simulated cases. This approach is analogous to a response surface analysis of data from an experiment where five quantitative experimental factors were altered according to a 3^5-factorial design and where the goal is to determine which factors significantly affect the response variable.[4]

To see if a response variable (LMV, say) was sensitive to an input parameter (k_b, say), a nonlinear, least squares regression model based on only the other four input parameters was calculated; that is, k_b was ignored when calculating the regression model for LMV. We calculated the correlation coefficient between each simulated LMV and the associated regression model predicted LMV for the four input parameter model, and we also calculated the list of absolute differences between each simulated and predicted LMV. If the correlation coefficient was nearly the same as for the original, five-input parameter model and the absolute differences were no larger for the four-parameter model, then one could conclude that LMV was insensitive to the parameter k_b. In other words, if LMV could be approximated just as well without including information about k_b, then LMV was said to be insensitive to k_b. On the other hand, if the correlation coefficient was notably smaller or the absolute differences larger than when all five parameters were used, one could conclude that LMV was sensitive to k_b.

RESULTS AND DISCUSSION

Case Studies

A typical time course of a single simulation is shown in Figure 2. The model predicted disinfection of the biofilm followed by regrowth once the biocide dose was over. Viable cell numbers and biofilm thickness reduction were dissimilar measures of biocide efficacy. For this illustrative case, viable cell numbers [Equation (24)] reached a minimum of 0.0014 at 3.0 h after the biocide dose whereas the minimum normalized thickness of only 0.23 occurred at 21.0 h. Such disparate results of different biocide efficacy assays have been reported by experimenters.[33] The general behavior predicted by the model is in good qualitative agreement with an experimental report of regrowth.[14]

As suggested by the simulation shown in Figure 2, disinfection exceeded removal. This was true in all 243 cases simulated. The minimum fractional reduction in viable cells, which reflects the sum of disinfection and removal process, ranged from 9×10^{-14} to 0.99 (geometric mean 3.6×10^{-5}) while the minimum normalized thickness, which reflects removal alone, ranged from 0.025 to 1.0 (geometric mean 0.40). This comparison indicates that, on average, there was a much greater reduction in viable cell numbers than there was in thickness. These simulation results are consistent with experimental observations of more rapid disinfection than detachment.[30,33]

The efficacy of biofilm disinfection was poor compared to the disinfection predicted for planktonic cells under the same treatment conditions. To quantify this comparison, the observed biofilm disinfection rate was ratioed to the disinfection rate predicted for planktonic cells exposed to the theoretical concentration of biocide assuming no consumption of biocide by reaction. Biofilm disinfection rate was expressed as an average first-order decay coefficient during the interval from biocide dose initiation to minimum value of viable cell areal density:

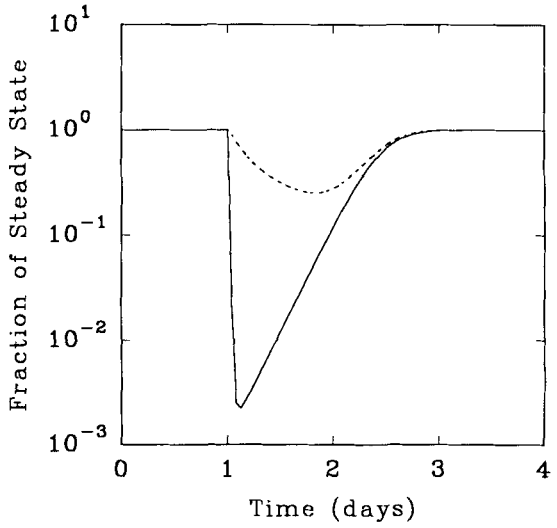

Figure 2. Biofilm disinfection and regrowth. Biocide was dosed into the reactor at a feed concentration of 4 g m^{-3} h at t_1 = 1 day. The response of biofilm thickness (----------) and viable cell areal density per Equation (24) (———) are shown.

$$\eta_b = \frac{[-1/(t_{\min} - t_1)] \ln (X_{vb}(t_{\min})/X^0_{vb})}{\exp(-k_b \int_{t_1}^{t_{\min}} C_b^* \, dt)} \quad (25)$$

where X_{vb}/X^0_{vb} is given by Equation (24) and the integral is found from the solution to a step change in a continuous stirred tank reactor (CSTR):

$$\int_{t_1}^{t_{\min}} C_b^* \, dt = C_b^i \left[(t_2 - t_1) - \exp(-\frac{Q}{V}(t_{\min} - t_1)) - \exp(-\frac{Q}{V}(t_{\min} - t_2)) \right] \quad (26)$$

The efficacy ratio η_b ranged from 6.4×10^{-4} to 0.79 (geometric mean 0.039); thus, biofilm microorganisms were, in some instances, orders of magnitude less susceptible than their planktonic counterparts. This difference probably reflects the fact that the biofilm consumes biocide by reaction.

Because the biocide reacts with biomass, it can be depleted in the bulk fluid of the reactor or in a gradient within the biofilm. To evaluate the relative contributions of these two modes of biocide depletion, the ratio of biocide concentrations at various points in the system after 1 h of biocide treatment was compared for all 243 cases (Fig. 3). The ratio C_b^s/C_b^* reflects the magnitude of the reduction in biocide concentration within the biofilm. This ratio ranged from 1.2×10^{-7} to 0.85 (geometric mean 4.1×10^{-3}). The ratio $C_b^*/0.3408C_{bi}$ indicates the magnitude of the reduction in biocide concentration in the bulk fluid; the factor of 0.3408 accounts for the maximum bulk fluid concentration for the step change in influent concentration neglecting reaction $[1 - \exp(-Q(t_2 - t_1)/V]$. This ratio ranged from 0.074 to 0.85 (geometric mean 0.30). This comparison shows that reduction in biocide concentration in the bulk fluid is typically less than one order of magnitude, whereas reduction in biocide concentration inside the biofilm can be profound. The nine clusters of points in Figure 3 represent the nine possible combinations of L_f and k_r values. Smaller values on either axis correspond to larger values of L_f and larger values of k_r.

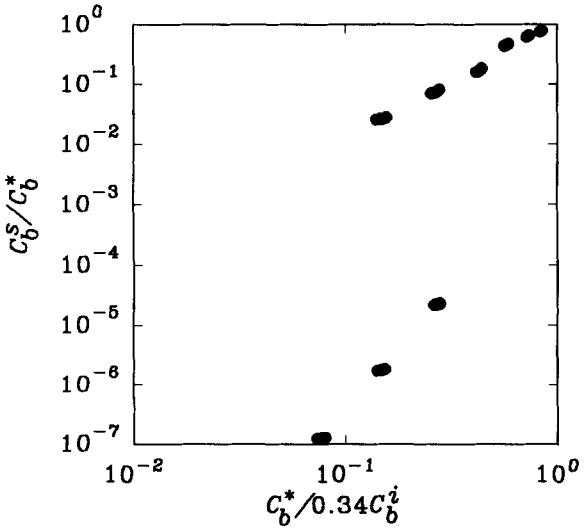

Figure 3. Biocide depletion in bulk fluid and biofilm. The y axis compares the ratio of the biocide concentrations at the substratum and in the bulk fluid after 1 h of biocide dosing. The x axis is the ratio of the actual biocide concentration in the bulk fluid to the calculated concentration that would be achieved after 1 h if there were no reaction of biocide.

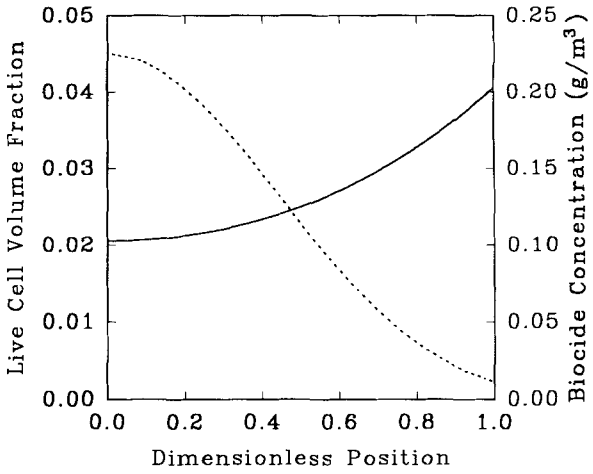

Figure 4. Gradients within biofilm during disinfection. The concentration of biocide (———), right axis, and viable cells (----------), left axis, are shown for after 1 h of disinfection. The parameter settings are the same as for Figure 2. On the x axis, $x = 0$ corresponds to the substratum and $x = 1$ to the biofilm–bulk fluid interface. The dimensional thickness of the biofilm was 44.4 μm.

The depletion of biocide within the biofilm stems from a reaction–diffusion interaction. The model predicts the biocide concentration gradient as well as the gradient in live cell fraction (Fig. 4). Biocide is at its highest concentration near the biofilm–bulk fluid interface and becomes reduced in the biofilm interior. In some cases, the biocide concentration at the substratum was less than 1% on the bulk fluid concentration. The profile of viable cell fraction is reversed: Cells survive in greatest numbers deep in the biofilm and are killed most effectively near the bulk fluid interface. Traditional engineering analyses of reaction–diffusion problems make use of the Thiele modulus, a dimensionless group that compares rates of reaction and diffusion. The biocide efficacy ratio η_b is plotted versus the Thiele modulus in Figure 5. This plot indicates that much of the variability in efficacy can be attributed to the reaction–diffusion interaction ($r^2 = 0.81$). Experimental support for the phenomenon of biocide diffusion limitation, at least for reactive biocides, is now emerging.[12,17,35]

Alternative biocide dosing protocols are readily evaluated using the model (Fig. 6). Repeated doses that are spaced farther apart than the 99% recovery time do not afford good biofilm control. The response pattern for a single dose (e.g., Fig. 2) is simply repeated in time; there is some fraction of the time when the biofilm is at or near its steady-state thickness. The response pattern to

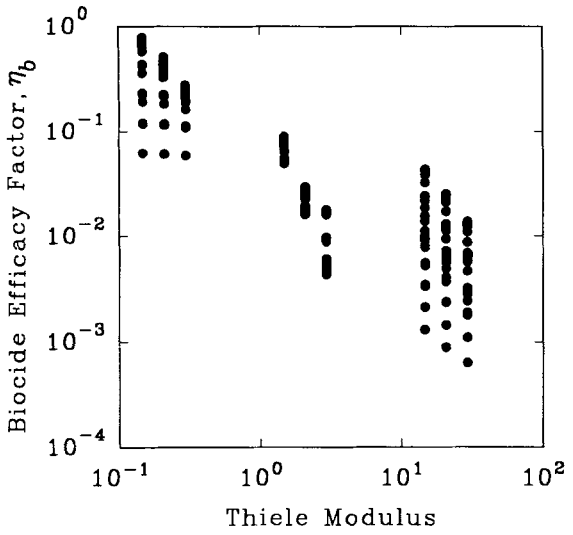

Figure 5. Biocide efficacy as a function of relative rates of reaction and diffusion. The Thiele modulus used is the conventional formulation for first-order kinetics, $\phi = (k_r \varepsilon_c \rho_x L_f^2 / \tau D_b)^{1/2}$.

periodic biocide dosing is reminiscent of experimental data collected in laboratory and pilot systems.[25] For example, when biocide was dosed for 1 h at 4 g m^{-3} every 3 days, the model showed that biofilm thickness averaged 74% of its steady-state value. When the same amount of biocide was applied in a different pattern, 1-h doses at 2 g m^{-3} every 1.5 days, the biofilm thickness averaged 71% of its steady-state value. The strong dependence of biocide efficacy on the Thiele modulus suggested that a more effective approach would be to challenge the biofilm when it is thinnest. A third simulation in which a 4-g m^{-3} dose of biocide was followed 0.8 days later by repeated doses of only 0.5 g m^{-3} gave good control (Fig. 6a). In this case, which involves less total biocide than the first two cases mentioned, the biofilm was reduced to approximately 2% of its initial thickness after 11 days of treatment. The optimal interval between the two doses in this simulation was 19 h (Fig. 6b), which coincides roughly with the time to minimum thickness (TMT) following the first dose of 21 h. These results indicate that the model could be a useful tool for designing optimal biocide delivery protocols. An important step in the continued development of the model will be systematic evaluation by comparison of model predictions with experimental data.

Sensitivity Analysis

Figure 7 is one of the 15 scatter plots constructed to visualize how each of the three response variables was associated with each of the five input parameters. Figure 7 shows the relationship between LMV and L_f. There are 81 points at each value of L_f, one point for each combination of the other four input parameters. The plot shows that LMV is very sensitive to L_f. If the initial biofilm is thin ($L_f = 5$ μm), then LMV varies over a wide range depending on the combination of the other four input parameters. But if the initial biofilm is thick ($L_f = 500$ μm), then LMV is nearly zero regardless of the values of the other four input parameters, at least for the ranges of parameter values used in this study. The response variables TMT and TR99 were similarly sensitive to L_f. No other interesting relationships were evident from the plots.

Each of the scatter plots in Figure 8 shows the relationship between a pair of response variables. Sometimes, in sensitivity analyses, such a scatter plot comprises clusters of points where each cluster is associated with a specific pattern of input parameter values. In this case, however, clusters are not evident. Instead the points in each plot form a smooth curve, indicating that

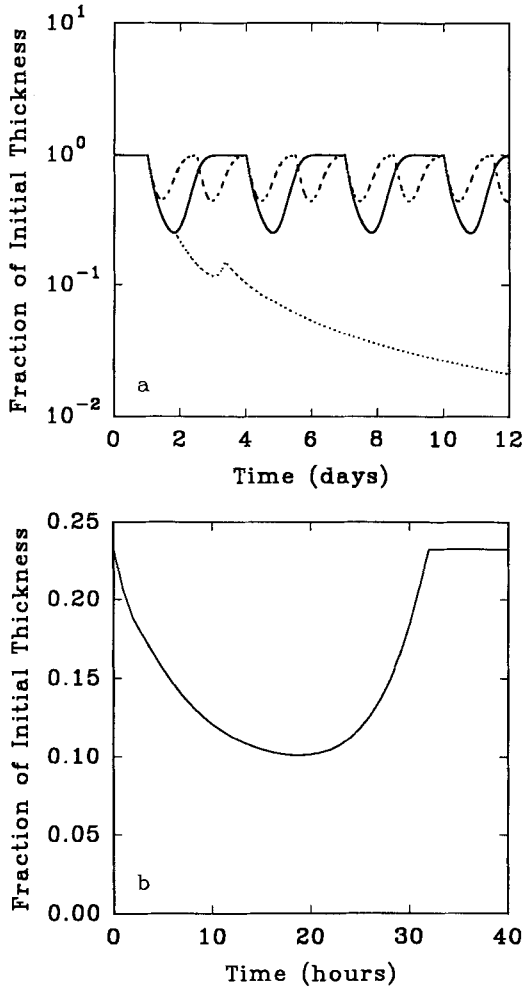

Figure 6. Alternative biocide dosage protocols. The normalized thickness, L_f/L_f^0, is plotted for three alternative repeated treatments (a) that begin at $t = 1$ day: 4 g m^{-3} for 1 h repeated every 3 days (———); 2 g m^{-3} for 1 h repeated every 1.5 days (----------); 4 g m^{-3} at $t = 1$ day, followed by 0.5 g m^{-3} for 1 h 0.8 days later, thereafter 0.5 g m^{-3} for 1 h every 1.5 days (·····). Other parameter values are the same as given in Figure 2. (b) Minimum fractional thickness achieved when a dose of 4 g m^{-3} for 1 h is followed by 0.5 g m^{-3} for 1 h after the interval indicated on the x axis.

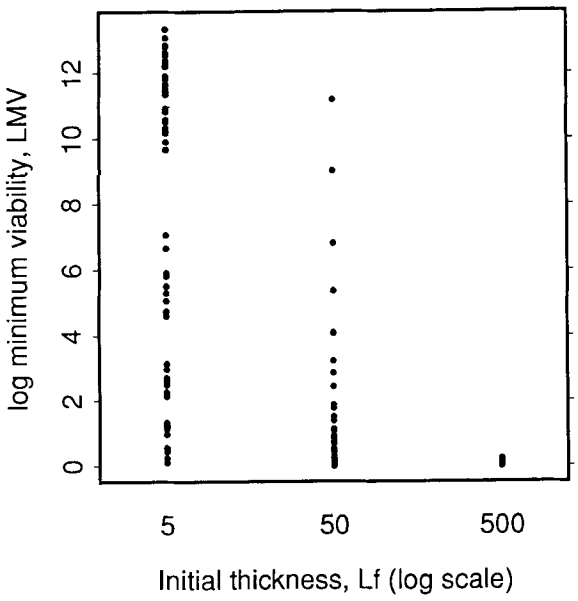

Figure 7. Dependence of LMV on L_f^0. There are 81 points above each of the three values of L_f^0, one point for each combination of the other four input variables.

the response variables are strongly associated. These relationships among the response variables were not evident to us from inspection of the governing equations. Because the association between TMT and TR99 is linear, except near zero, we choose to study the sensitivity of TMT to the input parameters, then extend the results to TR99 via the linear transformation, TR99 = 1.5 + 1.05TMT, which is nearly exact for TMT ≤ 0.5 days.

The regression model for LMV [Equation (27)] closely emulates the computer model for the 243 cases simulated in this investigation. The correlation coefficient is 0.996 between the LMV predicted by Equation (27) and the computer model simulated LMV.

$$\text{LMV} = \frac{12.9 \cdot H}{0.019 + H} \quad \text{where } H = \frac{k_b^{1.9} \cdot C_b^{1.8} \cdot t_b^{2.1}}{L_f^{2.2} \cdot k_r^{1.8}} \tag{27}$$

Note that L_f is in the denominator of H in Equation (27). If the initial biofilm thickness is large, then H is small, and correspondingly, LMV is small, in agreement with Figure 7.

Regression and correlation calculations were done five times to measure the sensitivity of LMV against each individual input parameter. For the four-parameter model without L_f, the correlation between predicted and simulated values dropped to 0.240, indicating that LMV is very sensitive to L_f. The correlations were 0.652, 0.881, 0.902, and 0.904 for the four-parameter models without k_b, without t_b, without k_r, and without C_b, respectively.

For each regression model, we formed the cumulative percentage curve of the 243 absolute differences between the simulated value and the predicted value based on the regression model. The curves are presented in Figure 9. For a cumulative percentage curve, the ordinate value is the percentage of the 243 absolute differences that are less than or equal to the corresponding differences on the abscissa. Clearly, the full regression model is best at predicting the simulated LMV values and the four-parameter model without L_f is worst, indicating that LMV is most sensitive to L_f. The regression model without k_b provides the next worst predictions; i.e., k_b is the second most influential input parameter. The remaining three four-parameter models have about the equivalent predictive ability; therefore, LMV is least sensitive to t_b, k_r, and C_b.

For the full model, 2.9% of the absolute differences are greater than 1; that is, for only 2.9% of the 243 cases, the full regression model prediction of minimum viability differs by at least an order of magnitude from the simulated minimum viability. Correspondingly, the

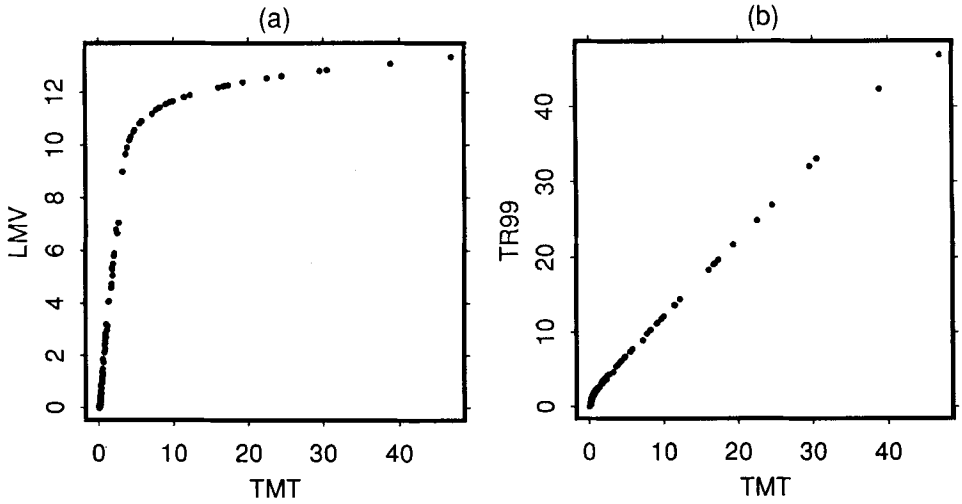

Figure 8. Relationships between response variables: (a) LMV as related to TMT and (b) TR99 as related to TMT. There are 243 points in each scatterplot, one point for each combination of the input variables. The relationship between LMV and TR99 is not shown because it is very similar to (a).

percentages of absolute differences greater than 1 are 70.8%, 38.7%, 22.6%, 21.0%, and 20.6% for the four-parameter models without L_f, without k_b, without t_b, without C_b, and without k_r, respectively. There percentages, which can be read to graphical accuracy from Figure 9, order the input parameters according to their influence on LMV.

We conclude from these analyses that LMV is most sensitive to L_f, next most sensitive to k_b, and less, but equally, sensitive to t_b, k_r, and C_b. The sensitivity of the system to biofilm thickness suggests that biofilm structural heterogeneity may be an important aspect of this problem. The sensitivity calculations for TMT and TR99 led to the same conclusions as for LMV; the details will not be presented.

CONCLUSIONS

The computer model described in this article captured several general features of antimicrobial agent action against biofilms that have been observed widely by experimenters and practitioners. These included (1) rapid disinfection followed by biofilm regrowth, (2) slower detachment than disinfection, and (3) reduced susceptibility of microorganisms in biofilms. The simulations support the plausibility of a mechanism of biofilm resistance in which the biocide is neutralized by reaction with biofilm constituents, leading to a reduction in the bulk biocide concentration and, more significantly, biocide concentration gradients within the biofilm.

The model will be useful for studying alternative biocide control strategies. The case study simulations suggested potentially effective strategies. In particular, the simulations suggest that a good interval between pulses of biocide is the time to minimum thickness (TMT) (Fig. 6b).

Sensitivity experiments and analyses identified which input parameters influence key response variables. For the range of input values of the experiment summarized above, each of the response variables (LMV, TMT, and TR99) was sensitive to each of five input parameters, but they were most sensitive to L_f and next most sensitive to k_b.

The simulations showed that the response variables are closely related; in fact, TR99 is linearly related to TMT. Statistical regression modeling produced simple equations for approximating the response variables for situations within the range of conditions covered by the sensitivity experiment. Within the domain of the simulation study, the regression model can be used to suggest optimum values of the control parameters C_b and t_b if accurate estimates of key input parameters are available.

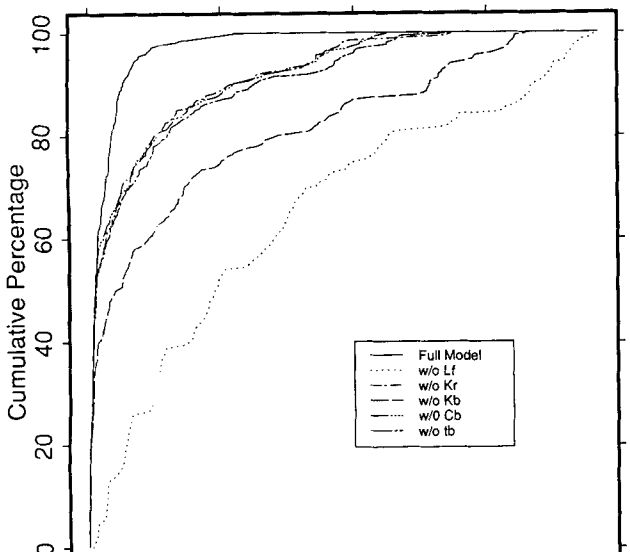

Figure 9. Comparison of complete and incomplete regression models. For each of six regression models, the cumulative percentage plot of absolute errors between the regression prediction of LMV and the computer model simulated value is traced. The full model is Eq. (27). Each of the other five models is of the same functional form as Eq. (27) except that one of the input variables is dropped from the model and the constants and exponents are adjusted to give the best possible prediction according to nonlinear least squares regression analysis. Each cumulative percentage plot is based on 243 absolute errors, one error for each combination of the five input variables.

This work was supported by the Center for Biofilm Engineering at Montana State University, a National Science Foundation supported Engineering Research Center (cooperative agreement EEC-8907039), and by the Center's Industrial Associates.

NOMENCLATURE

A	biofilm surface area (m^2)
b	death rate coefficient (d^{-1})
C_b	concentration of biocide (g m^{-3})
C_s	concentration of substrate (g m^{-3})
D_b	diffusion coefficient of biocide in water (m^2 d^{-1})
D_s	diffusion coefficient of substrate in water (m^2 d^{-1})
k_b	biocide disinfection rate coefficient (m^3 g^{-1} d^{-1})
k_d	detachment rate coefficient (m^{-1} d^{-1})
k_r	biocide reaction rate coefficient (m^3 g^{-1} d^{-1})
K_s	substrate Monod half-saturation coefficient (g m^{-3})
L_f	biofilm thickness (m or μm)
LMV	$\log_{10}$ minimum normalized viable cell areal density
Q	volumetric flow rate (m^3 d^{-1})
r	Pearson product–moment correlation coefficient
t	time (d)
t_b	duration of biocide dose, $t_b = t_2 - t_1$ (d)
t_1	time of initiation of biocide dose (d)
t_2	time of cessation of biocide dose (d)
t_{min}	time of minimum viable cell areal density (d)
TMT	time to minimum biofilm thickness after initiation of biocide dose (h)
TR99	time to recovery of biofilm thickness to 99% of initial thickness after initiation of biocide dose (h)
v	cell advective velocity (m d^{-1})
V	volume of bulk liquid compartment (m^3)

X_a concentration of live cells in suspension (g m^{-3})
X_i concentration of dead cells in suspension (g m^{-3})
X_{vb} live cell biofilm areal density (g m^{-2})
Y_{xs} yield coefficient of biomass on substrate (g g^{-1})
z distance coordinate normal to the substratum (m)

Greek Letters

ε_a live cell volume fraction
ε_c cell fraction of total biofilm volume
ε_i dead cell volume fraction
η_b biocide efficacy ratio
μ_{max} maximum specific growth rate (d^{-1})
ρ_x cell intrinsic density (g m^{-3})
τ biofilm/bulk fluid effective diffusivity ratio
ϕ Thiele modulus

Superscripts

^{i} influent value
^{0} initial value
^{s} value at substratum, $z = 0$
* bulk fluid value

References

1. Al-Holti, B., Waite, T., Chow, W. 1990. Development and calibration of a model for predicting optimum chlorination scenarios for biofouling control. pp. 521–534. In. R. L. Jolley et al. (eds.), Water chlorination: Chemistry, environmental impact and health effects, vol. 6. Lewis Publishers, Chelsea, MI.
2. Bailey, J. E., Ollis, D. F. 1986. Biochemical engineering fundamentals. McGraw-Hill, New York.
3. Biswas, P., Lu, C., Clark, R. M. 1993. A model for chlorine concentration decay in drinking water distribution pipes. Wat. Res. **27**: 1715–1724.
4. Box, G. E. P., Hunter, W. G., Hunter, J. S. 1978. Statistics for experimenters. Wiley, New York.
5. Brandstetter, A., Buxton, B. E. 1987. The role of geostatistical, sensitivity, and uncertainty analysis in performance assessment. pp. 96–110. In: Geostatistical, sensitivity, and uncertainty methods for ground-water flow and radionuclide transport modeling. Battelle Press, Columbus, OH.
6. Camper, A. K. 1993. Coliform regrowth and biofilm accumulation in drinking water systems: A review. pp. 91–105. In: G. G. Geesey, Z. Lewandowski, and H.-C. Flemming (eds.), Biofouling and biocorrosion in industrial water systems. Lewis Publishers, Boca Raton, FL.
7. Carpentier, B., Cerf, O. 1993. Biofilms and their consequences, with particular reference to hygiene in the food industry. J. Appl. Bacteriol. **75**: 499–511.
8. Characklis, W. G. 1990. Microbial biofouling control. pp. 585–633. In: W. G. Characklis and K. C. Marshall (eds.), Biofilms. J Wiley, New York.
9. Chen, C.-I., Griebe, T., Characklis, W. G. 1993. Biocide action of monochloramine on biofilm systems of *Pseudomonas aeruginosa*. **7**: 1–17.
10. Chen, C.-I., Griebe, T., Srinivasan, R., Stewart, P. S. 1993. Effects of various metal substrata on accumulation of *Pseudomonas aeruginosa* biofilms and the efficacy of monochloramine as a biocide. Biofouling **7**: 241–251.
11. Costerton, J. W., Cheng, K.-J., Geesey, G. G., Ladd, T. I., Nickel, J. C., Dasgupta, M., Marrie, T. J. 1987. Bacterial biofilms in nature and disease. Ann. Rev. Microbiol. **41**: 435–464.
12. de Beer, D., Srinivasan, R., Stewart, P. S. 1994. Direct measurement of chlorine penetration into biofilms during disinfection. Appl. Environ. Microbiol. **60**: 4339–4344.
13. Eastwood, I. M. 1994. Problems with biocides and biofilms. In: J. Wimpenny, W. Nichols, D. Stickler, and H. Lappin-Scott (eds.), Bacterial biofilms and their control in medicine and industry. BioLine, Cardiff, United Kingdom.
14. Griebe, T., Chen, C.-I., Srinivasan, R., Stewart, P. S. 1994. Analysis of biofilm disinfection by monochloramine and free chlorine. pp. 151–161. In: G. G. Geesey, Z. Lewandowski, and H.-C. Flemming (eds.), Biofouling and biocorrosion in industrial water systems. Lewis Publishers, Boca Raton, FL.
15. Herbert, B. N. 1994. Biofilms and pipelines. In: J. Wimpenny, W. Nichols, D. Stickler, and H. Lappin-Scott (eds.), Bacterial biofilms and their control in medicine and industry. BioLine, Cardiff, United Kingdom.
16. Holt, D. M. 1987. Microbiology of paper and board manufacture. pp. 493–506. In: D. R. Houghton et al. (eds.), Biodeterioration, vol. 7. Elsevier Applied Science, London.
17. Huang, C.-T., Yu, F. P., McFeters, G. A., Stewart, P. S. 1995. Nonuniform spatial patterns of respiratory activity within biofilm during disinfection. Appl. Environ. Microbiol. **61**: 2252–2256.
18. Iman, R. L., Helton, J. C., Campbell, J. E. 1981. An approach to sensitivity analysis of computer models: Part 1—introduction, input variable selection and preliminary variable assessment. J. Qual. Technol. **13**: 174–183.
19. Iman, R. L., Helton, J. C., Campbell, J. E. 1981. An approach to sensitivity analysis of computer models: Part II—ranking of input variables, response surface validation, distribution effect and technique synopsis. J. Qual. Technol. **13**: 232–240.
20. Kinniment, S. L., Wimpenny, J. W. T. 1992. Biocide testing on biofilm derived from metalworking fluids. Quart. J. Tech. Papers, October, p. 43.
21. Kissel, J. C., McCarty, P. L., Street, R. L. 1984. Numerical simulation of mixed-culture biofilm. J. Environ. Eng. (ASCE) **110**: 393.
22. Marsh, P., Martin, M. 1984. Oral microbiology. Van Nostrand and Reinhold, Wokingham, Berkshire, United Kingdom.
23. Nichols, W. W. 1989. Susceptibility of biofilms to toxic compounds. pp. 321–331 In: W. G. Characklis and P. A. Wilderer, (eds.), Structure and function of biofilms. Wiley, New York.
24. Nichols, W. W., Evans, M. J., Slack, M. P. E., Walmsley, H. L. 1989. The penetration of antibiotics into aggregates of mucoid and non-mucoid *Pseudomonas aeruginosa*. J. Gen. Microbiol. **135**: 1291–1303.
25. Novak, L. 1982. Comparison of the Rhine river and the Öresund sea water fouling and its removal by chlorination. J. Heat Trans. **104**: 663–669.
26. Perry, R. H., Chilton, C. H. 1973. Chemical engineer's handbook, 5th ed. McGraw-Hill, New York.
27. Ridgway, H. F., Rigby, M. G., Argo, D. G. 1985. Bacterial adhesion and fouling of reverse osmosis membranes. J. AWWA **7**(7): 97–106.
28. Robinson, J. A., Trulear, M. G., Characklis, W. G. 1984. Cellular reproduction and extracellular polymer formation by *Pseudomonas aeruginosa* in continuous culture. Biotechnol. Bioeng. **26**: 1409–1417.
29. Rossmann, L. A., Clark, R. M., Grayman, W. M. 1994. Modeling chlorine residuals in drinking water distribution systems. J. Environ. Eng. **120**: 803–820.
30. Srinivasan, R., Stewart, P. S., Griebe, T., Chen, C.-I., Xu, X. 1995. Biofilm parameters influencing biocide efficacy. Biotechnol. Bioeng. **46**: 553–560.
31. Stewart, P. S. 1993. A model of biofilm detachment. Biotechnol. Bioeng. **41**: 111–117.
32. Stewart, P. S. 1994. Biofilm accumulation model that predicts antibiotic resistance of *Pseudomonas aeruginosa* biofilms. Antimicrob. Agents Chemother. **38**: 1052–1058.
33. Stewart, P. S., Griebe, T., Srinivasan, R., Chen, C.-I., Yu, F. P., deBeer, D., McFeters, G. A. 1994. Comparison of respiratory activity and culturability during monochloramine disinfection of binary population biofilms. Appl. Environ. Microbiol. **60**: 1690–1692.

34. Strauss, S. D., Puckorius, P. R. 1984. Cooling-water treatment for control of scaling, fouling, corrosion. Power **128**: S1–S24.
35. Tashiro, H., Numakura, T., Nishikawa, S., Miyaji, Y. 1991. Penetration of biocides into biofilms. Wat. Sci. Technol. **23**: 1395–1403.
36. Wanner, O., Gujer, W. 1986. A multispecies biofilm model. Biotechnol. Bioeng. **28**: 314–328.
37. Westrin, B. A., Axelsson, A. 1991. Diffusion in gels containing immobilized cells: A critical review. Biotechnol. Bioeng. **38**: 439–446.